

Reflection asymmetry and triaxiality in even-even atomic nuclei

Nikolay Minkov
(Николай Минков)

Institute of Nuclear Research and Nuclear Energy
Bulgarian Academy of Sciences, Sofia, Bulgaria
Research Group on Complex Deformed Atomic Nuclei



CWAN'23, Huizhou, 11 July 2023

Contents

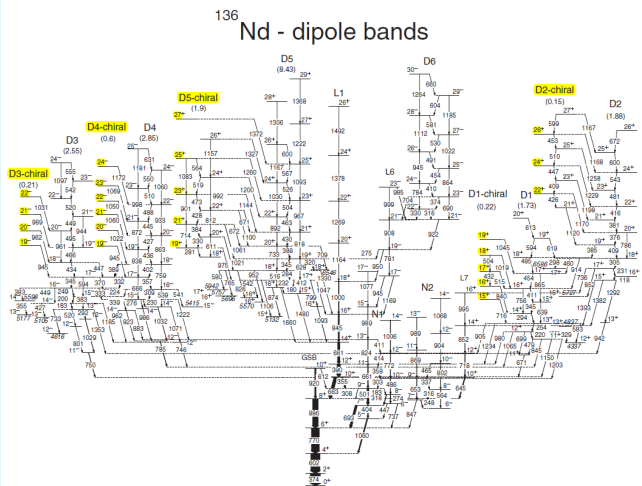
- 1 Coexistence of quadrupole triaxial and octupole shapes
- 2 Quadrupole-octupole shapes and spectra
- 3 Quadrupole-octupole rotation model (QORM)
 - Probing octupole collectivity in ^{136}Nd
 - Spectra of recognized quadrupole-octupole deformed nuclei
 - Indications for high-spin quadrupole-octupole triaxiality
- 4 Conclusion



Chiral structure of experimental energy bands in ^{136}Nd

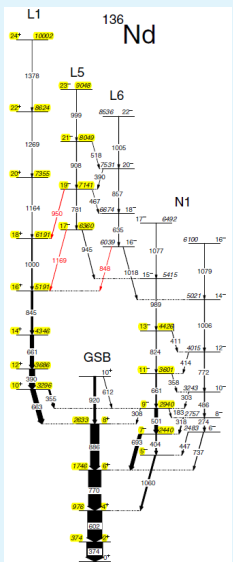
EVOLUTION FROM γ -SOFT TO STABLE ...

PHYSICAL REVIEW C 98, 044304 (2018)



C. Petrache et al.

Alternating-parity band (APB) structures in ^{136}Nd



C. Petrache, N.M., et al.
PRC **102**, 014311 (2020)

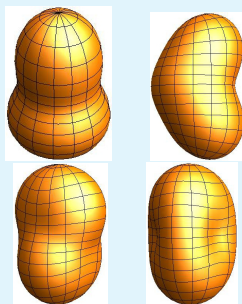
Coexistence of chiral/triaxial and octupole shapes

OBSERVATIONS:

- Chiral/triaxial and octupole shapes can coexist in certain nuclear regions.
- Octupole shapes in even-even nuclei manifest in the form of alternating-parity bands (APB).
- APBs are mainly attributed to axial (pear-shape) quadrupole-octupole (QO) deformation.

QUESTION: Could the APB indicate itself the presence of a triaxial QO deformation?

Quadrupole-Octupole Shapes



[P. Butler and W. Nazarewicz, RMP **68**,
349 (1996)]

$$\beta_{20}=0.65 \quad \beta_{3\mu}=0.35$$

body-fixed coordinates

$$\alpha_{\lambda\mu} \rightarrow \beta_{\lambda,\mu}$$

$$(\mu = 0, 1, 2, 3)$$

$$R(\theta, \varphi) = R_0 \left(1 + \sum_{\lambda=2,3} \sum_{\mu=-\lambda}^{\lambda} \alpha_{\lambda\mu} Y_{\lambda\mu}^*(\theta, \varphi) \right)$$

Shell model origin of octupole deformation

- Coupling of orbitals with different parity and ($\Delta I = 3$) near the Fermi level $\rightarrow (N, I, j) \otimes (N - 1, I - 3, j - 3)$
- Particle numbers favouring strong octupole correlations

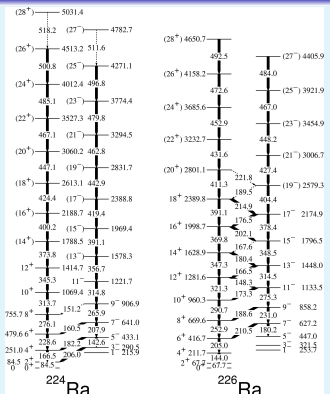
$$\mathbf{34} (g_{\frac{9}{2}} \otimes p_{\frac{3}{2}}) \quad \mathbf{56} (h_{\frac{11}{2}} \otimes d_{\frac{5}{2}}) \quad \mathbf{88} (i_{\frac{13}{2}} \otimes f_{\frac{7}{2}}) \quad \mathbf{134} (j_{\frac{15}{2}} \otimes g_{\frac{9}{2}})$$

\Rightarrow regions of pronounced octupole deformations/collectivity

^{144}Ba ($Z = 56$, $N = 88$) \Rightarrow Xe ($Z=54$) – Ba ($Z=56$) – Ce ($Z=58$)

^{222}Ra ($Z = 88$, $N = 134$) \Rightarrow Rn ($Z=86$) – Ra ($Z=88$) – Th ($Z=90$)

Alternating-parity bands (APBs) at stable octupole mode



J. F. C. Cocks et al

PRL 78, 2920 (1997)

Recent confirmations of GS octupole deformation:

^{224}Ra – L. Gaffney et al, Nature 497, 199 (2013); P. Butler, JPG 43, 073002 (2016)

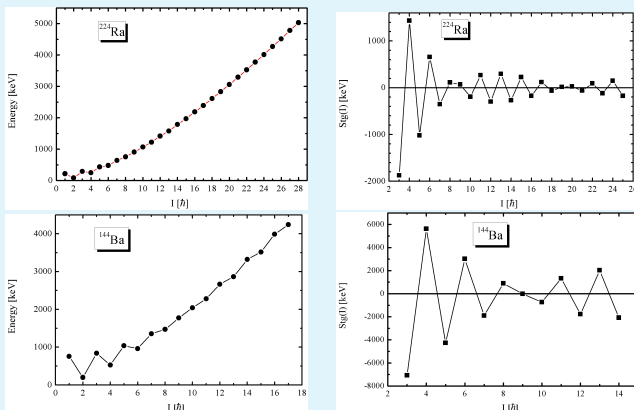
$^{144,146}\text{Ba}$ – B. Bucher et al, PRL 116, 112503 (2016); PRL 118, 152504 (2017)

New data expected:

^{142}Ba , $^{222,224,226}\text{Rn}$ and $^{222,228}\text{Ra}$ – P. Butler, L. Gaffney et al – HIE-ISOLDE

^{140}Ba – T. Mertzimekis et al – IFIN-HH

Fine staggering effects in APB (octupole) bands



$$\text{Stg}(I) = 6\Delta E(I) - 4\Delta E(I-1) - 4\Delta E(I+1) + \Delta E(I+2) + \Delta E(I-2)$$

$$\Delta E(I) = E(I+1) - E(I)$$

$I < 10 - 12 \rightarrow$ octupole vibration and collective rotation

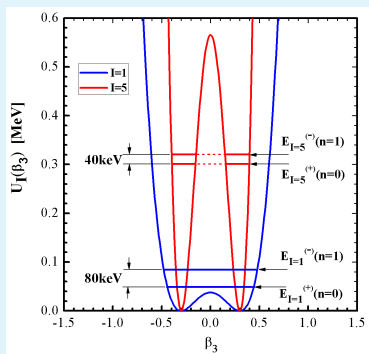
$I > 12 \rightarrow$ rotation of a stable quadrupole-octupole shape

Model of octupole vibrations and quadrupole-octupole rotations

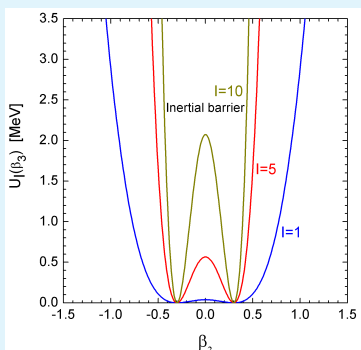
[N. M., S. Drenska, P. Yotov and W. Scheid, JPG 32, 497(2006)]

$$H_{\text{osc}}^{\text{oct}} = -\frac{\hbar^2}{2B_3} \frac{d^2}{d\beta_3^2} + U_I(\beta_3)$$

$$U(\beta_3, I) = \frac{1}{2} C(I) \beta_3^2 + \frac{I(I+1)}{2(d_2 + d_3 \beta_3^2)} \quad C(I) = \frac{2X(I)d_3}{(d_2 + d_3 \beta_{3 \min}^2)^2}$$

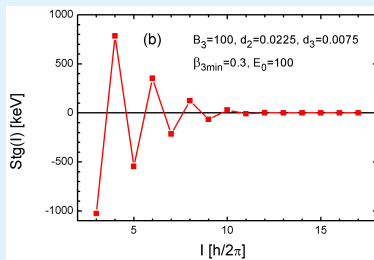
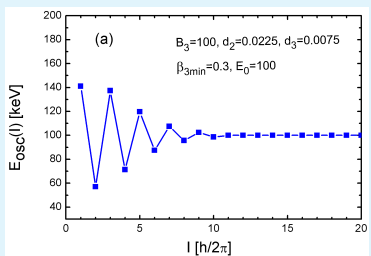


$I=\text{odd}$
 $I=\text{even}$



$$\pi(-1)^I = 1 \quad E_{\text{vib}}^{\text{oct}} = E_0 - \frac{1}{2}(-1)^I [E_I^{(-)} - E_I^{(+)}]$$

Energy and parity shift from double-well potential



Low-spin parity shift effect

Parametrization of the octupole shape. Octahedron symmetry

$$V_3 = \sum_{\mu=-3}^3 \alpha_{3\mu}^{\text{fix}} Y_{3\mu}^* \rightarrow \epsilon_0 A_2 + \sum_{i=1} \epsilon_1(i) F_1(i) + \sum_{i=1} \epsilon_2(i) F_2(i) \quad [\text{I. Hamamoto et al, 1991}]$$

$$A_2 = -\frac{i}{\sqrt{2}}(Y_{32} - Y_{3-2}) = \frac{1}{r^3} \sqrt{\frac{105}{4\pi}} xyz$$

$$F_1(1) = Y_{30} = \frac{1}{r^3} \sqrt{\frac{7}{4\pi}} z(z^2 - \frac{3}{2}x^2 - \frac{3}{2}y^2)$$

$$F_1(2) = -\frac{1}{4}\sqrt{5}(Y_{33} - Y_{3-3}) + \frac{1}{4}\sqrt{3}(Y_{31} - Y_{3-1})$$

$$= \frac{1}{r^3} \sqrt{\frac{7}{4\pi}} x(x^2 - \frac{3}{2}y^2 - \frac{3}{2}z^2)$$

$$F_1(3) = -i\frac{1}{4}\sqrt{5}(Y_{33} + Y_{3-3}) - i\frac{1}{4}\sqrt{3}(Y_{31} + Y_{3-1})$$

$$= \frac{1}{r^3} \sqrt{\frac{7}{4\pi}} y(y^2 - \frac{3}{2}z^2 - \frac{3}{2}x^2)$$

$$F_2(1) = \frac{1}{\sqrt{2}}(Y_{32} + Y_{3-2}) = \frac{1}{r^3} \sqrt{\frac{105}{16\pi}} z(x^2 - y^2)$$

$$F_2(2) = \frac{1}{4}\sqrt{3}(Y_{33} - Y_{3-3}) + \frac{1}{4}\sqrt{5}(Y_{31} - Y_{3-1}) = \frac{1}{r^3}\sqrt{\frac{105}{16\pi}}x(y^2 - z^2)$$

$$F_2(3) = -i\frac{1}{4}\sqrt{3}(Y_{33} + Y_{3-3}) + i\frac{1}{4}\sqrt{5}(Y_{31} + Y_{3-1}) = \frac{1}{r^3}\sqrt{\frac{105}{16\pi}}y(z^2 - x^2)$$

Quadrupole-octupole rotation Hamiltonian. Octahedron symmetry

[N. M. et al, PRC **63**, 044305 (2001)]

$$\hat{H}_{\text{qorm}} = \hat{H}_{\text{quad}} + \hat{H}_{\text{oct}} + \hat{H}_{\text{qoc}}$$

$$\hat{H}_{\text{oct}} = \hat{H}_{A_2} + \sum_{r=1}^2 \sum_{i=1}^3 \hat{H}_{F_r(i)}$$

$$\hat{H}_{A_2} = a_2 \frac{1}{4} [(\hat{l}_x \hat{l}_y + \hat{l}_y \hat{l}_x) \hat{l}_z + \hat{l}_z (\hat{l}_x \hat{l}_y + \hat{l}_y \hat{l}_x)]$$

$$\hat{H}_{F_1(1)} = \frac{1}{2} f_{11} (5 \hat{l}_z^3 - 3 \hat{l}_z \hat{l}^2)$$

$$\hat{H}_{F_2(1)} = f_{21} \frac{1}{2} [\hat{l}_z (\hat{l}_x^2 - \hat{l}_y^2) + (\hat{l}_x^2 - \hat{l}_y^2) \hat{l}_z]$$

$$\hat{H}_{F_1(2)} = \frac{1}{2} f_{12} (5 \hat{l}_x^3 - 3 \hat{l}_x \hat{l}^2)$$

$$\hat{H}_{F_2(2)} = f_{22} (\hat{l}_x \hat{l}^2 - \hat{l}_x^3 - \hat{l}_x \hat{l}_z^2 - \hat{l}_z^2 \hat{l}_x)$$

$$\hat{H}_{F_1(3)} = \frac{1}{2} f_{13} (5 \hat{l}_y^3 - 3 \hat{l}_y \hat{l}^2)$$

$$\hat{H}_{F_2(3)} = f_{23} (\hat{l}_y \hat{l}_z^2 + \hat{l}_z^2 \hat{l}_y + \hat{l}_y^3 - \hat{l}_y \hat{l}^2)$$

$$\hat{H}_{\text{quad}} = A \hat{l}^2 + A' \hat{l}_z^2 + C' (\hat{l}_x^2 - \hat{l}_y^2)$$

$$\hat{H}_{\text{qoc}} = f_{\text{qoc}} \frac{1}{l^2} (15 \hat{l}_z^5 - 14 \hat{l}_z^3 \hat{l}^2 + 3 \hat{l}_z \hat{l}^4)$$

Quadrupole-octupole rotation Hamiltonian. Octahedron symmetry

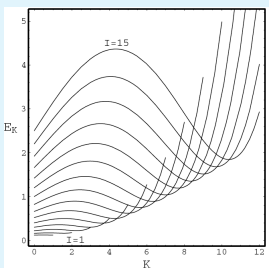
$$\hat{H}_{\text{qorm}} = \hat{H}_{\text{quad}} + \hat{H}_{\text{oct}} + \hat{H}_{\text{qoc}}$$

$$\hat{H}_{\text{oct}} = \hat{H}_{A_2} + \sum_{r=1}^2 \sum_{i=1}^3 \hat{H}_{F_r(i)}$$

Point-symmetry contents: $\hat{H}_{F_1(1)} \rightarrow Y_{30} \rightarrow \text{D}_\infty$; $\hat{H}_{F_1(2)} \rightarrow (Y_{31} - Y_{3-1}) \rightarrow \text{C}_{2v}$;

$\hat{H}_{F_2(1)} \rightarrow (Y_{32} + Y_{3-2}) \rightarrow \text{T}_d$; $\hat{H}_{F_2(2)} \rightarrow (Y_{33} - Y_{3-3}) \rightarrow \text{D}_{3h}$ [Octahedron irreps]

$$\begin{aligned} E_K^{\text{qorm}}(I) &= AI(I+1) + A'K^2 + (1/2)f_{11} [5K^3 - 3KI(I+1)] \\ &+ f_{\text{qoc}}(1/I^2) [15K^5 - 14K^3I(I+1) + 3KI^2(I+1)^2] \end{aligned}$$



$K_{\min} \rightarrow$ high-spin “beat” staggering effect
 [N. M. et al, PRC **63**, 044305 (2001); JPG **32**, 497(2006)]

Total QO rotation and vibration energy

⇒ Octupole vibration and quadrupole-octupole rotation

$$E_{\text{coll}} = E_{\text{vib}}^{\text{oct}} + E_{\text{qorm}}$$

⇒ **strong parity shift effect** at low angular momenta

⇒ **beat staggering patterns** in the higher energy regions

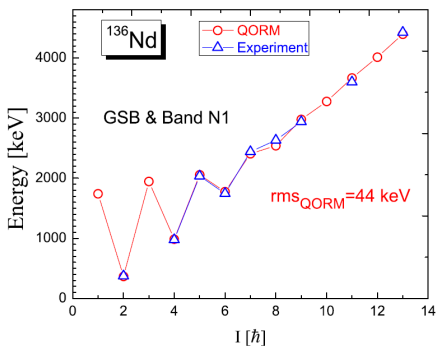
Probing octupole collectivity in ^{136}Nd Probing QORM description of ^{136}Nd APB [C. Petrache, N.M. et al.
PRC 102, 014311 (2020)]C. M. PETRACHE *et al.*

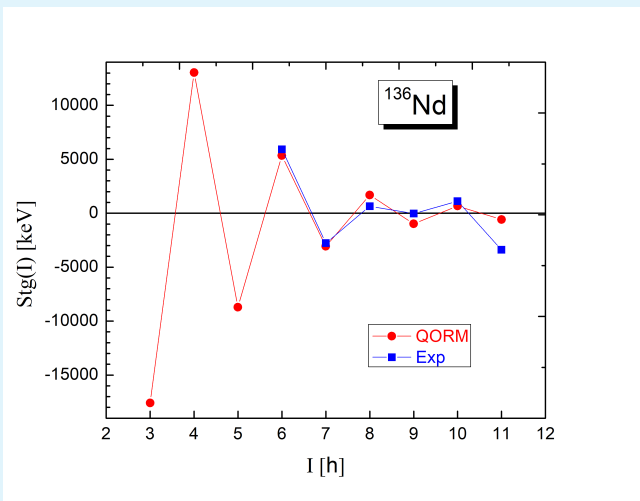
PHYSICAL REVIEW C 102, 014311 (2020)

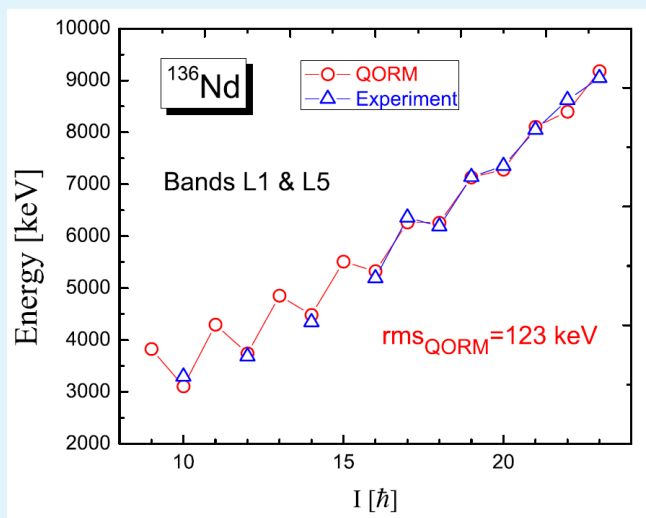
TABLE III. Experimental and QORM-calculated energies of the levels of the GSB (positive parity) and band $N1$ (negative parity) of ^{136}Nd .

I^π	E_{theory} (keV)	E_{exp} (keV)	$E_{\text{theory}} - E_{\text{exp}}$ (keV)
1 ⁻	1740	—	—
2 ⁺	367	374	-7
3 ⁻	1945	—	—
4 ⁺	985	976	9
5 ⁻	2057	2036	21
6 ⁺	1776	1746	30
7 ⁻	2408	2440	-32
8 ⁺	2540	2633	-93
9 ⁻	2978	2940	38
10 ⁺	3276	—	—
11 ⁻	3666	3601	65
12 ⁺	4013	—	—
13 ⁻	4396	4426	-30

the model and its application are given in Ref. [32]). We chose

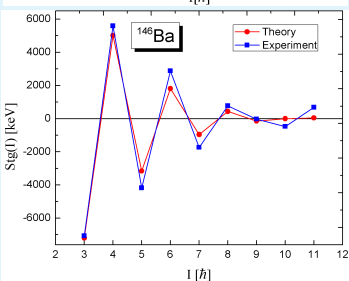
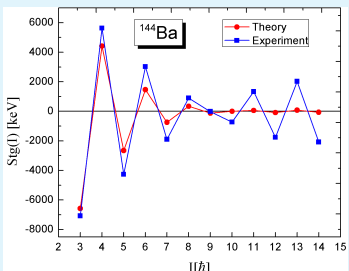
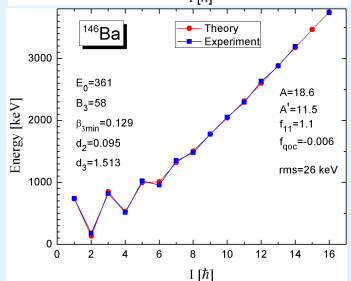
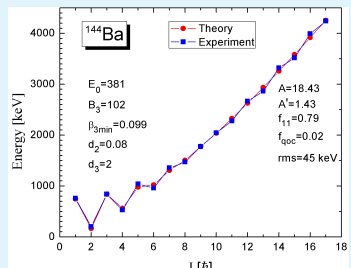
FIG. 6. QORM description of ^{136}Nd APB formed by GSB up to $I = 8^+$ and band $N1$ up to $I = 13^-$. See the text for the model parameters and explanation.

Experimental and theoretical staggering patterns for ^{136}Nd APB

Experimental and theoretical levels of the non-yrast APB in ^{136}Nd 

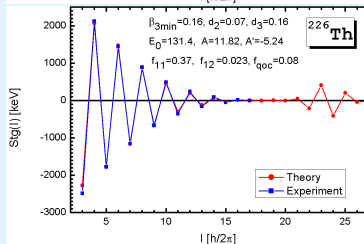
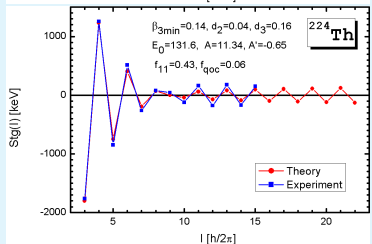
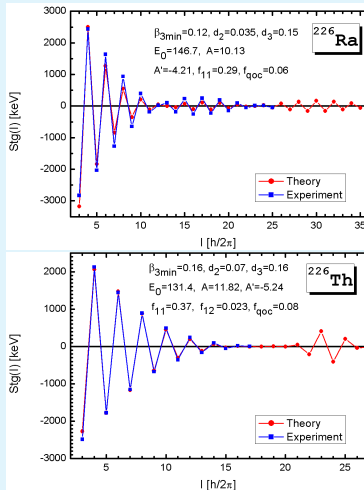
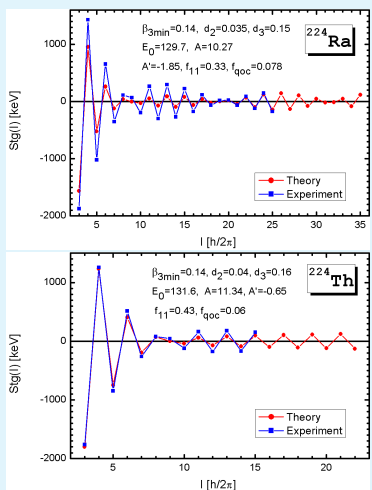


Spectra of recognized quadrupole-octupole deformed nuclei

 $^{144,146}\text{Ba}$: QORM description

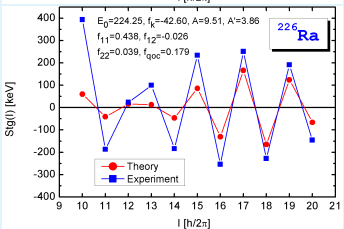
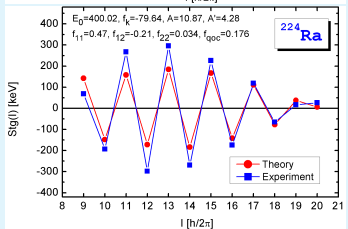
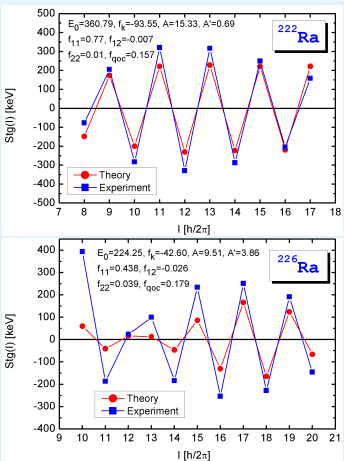
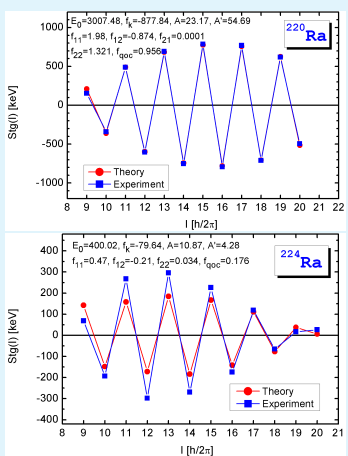
Spectra of recognized quadrupole-octupole deformed nuclei

“Beat” staggering patterns in Ra and Th nuclei



[N. M., P. Yotov, S. Drenska and W. Scheid, JPG 32, 497 (2006)]

Indications for high-spin quadrupole-octupole triaxiality

QORM application to high-spin APB regions \Rightarrow QO triaxiality

- ✓ Well reproduced high-spin beat staggering effect
- ✓ Rotation of stable quadrupole-octupole shape
- ✓ Contribution of non-axial Hamiltonian terms

Conclusion

- ^{136}Nd data: Possible coexistence of quadrupole triaxial/chiral and quadrupole-octupole collective degrees of freedom.
- QORM description of ^{136}Nd APB: Support of its quadrupole-octupole character.
- QORM description of high-spin APB structure in Ra isotopes: Indications for high-spin quadrupole-octupole triaxiality.
- Need for detailed study of high-spin APB structure in wider range of nuclei.
- Need for unified study of triaxiality and reflection asymmetry.